BAMS Article

An Intuitive Metric to Quantify and Communicate Tropical Cyclone Rainfall Hazard

Christopher D. Bosma, Daniel B. Wright, Phu Nguyen, James P. Kossin, Derrick C. Herndon, and J. Marshall Shepherd

ABSTRACT: Recent tropical cyclones (TCs) have highlighted the hazards that TC rainfall poses to human life and property. These hazards are not adequately conveyed by the commonly used Saffir–Simpson scale. Additionally, while recurrence intervals (or, their inverse, annual exceedance probabilities) are sometimes used in the popular media to convey the magnitude and likelihood of extreme rainfall and floods, these concepts are often misunderstood by the public and have important statistical limitations. We introduce an alternative metric—the extreme rain multiplier (ERM), which expresses TC rainfall as a multiple of the climatologically derived 2-yr rainfall value. ERM allows individuals to connect ("anchor," in cognitive psychology terms) the magnitude of a TC rainfall event to the magnitude of rain events that are more typically experienced in their area. A retrospective analysis of ERM values for TCs from 1948 to 2017 demonstrates the utility of the metric as a hazard quantification and communication tool. Hurricane Harvey (2017) had the highest ERM value during this period, underlining the storm's extreme nature. ERM correctly identifies damaging historical TC rainfall events that would have been classified as "weak" using wind-based metrics. The analysis also reveals that the distribution of ERM maxima is similar throughout the eastern and southern United States, allowing for both the accurate identification of locally extreme rainfall events and the development of regional-scale (rather than local-scale) recurrence interval estimates for extreme TC rainfall. Last, an analysis of precipitation forecast data for Hurricane Florence (2018) demonstrates ERM's ability to characterize Florence's extreme rainfall hazard in the days preceding landfall.

https://doi.org/10.1175/BAMS-D-19-0075.1
Corresponding author: Daniel B. Wright, danielb.wright@wisc.edu
In final form 28 October 2019

AFFILIATIONS: Bosma and Wright—Department of Civil and Environmental Engineering, University of Wisconsin–Madison, Madison, Wisconsin; Nguyen—Department of Civil and Environmental Engineering, University of California, Irvine, Irvine, California; Kossin—Center for Weather and Climate, NOAA/National Centers for Environmental Information, Madison, Wisconsin; Herndon—Cooperative Institute for Meteorological Satellite Studies, University of Wisconsin–Madison, Madison, Wisconsin; Shepherd—Program in Atmospheric Sciences, Department of Geography, University of Georgia, Athens, Georgia

Intense rainfall associated with tropical cyclones (TC) is a significant hazard to human life and property. From 1963 to 2012, extreme rainfall was the most frequent cause of tropical cyclone–related fatalities in the United States (Rappaport 2014). Climate models have indicated, with high confidence, that TC rainfall rates in the North Atlantic will increase due the effects of global warming (Knutson et al. 2010; USGCRP 2017), with projected increases of 5%–20% (Walsh et al. 2016). Furthermore, the mean translational speed of North Atlantic TCs over land has decreased by 20% since the mid-twentieth century (Kossin 2018). These changes have important implications since more intense, slower-moving storms are more likely to linger for long durations and to generate extreme rainfall totals.

The widely used Saffir–Simpson scale assigns TCs a hazard category from 1 to 5 based on maximum sustained wind speed, with category 5 being the most catastrophic. However, maximum wind speed is a not a reliable indicator of overall hazard. Six of the 10 deadliest TCs in the United States in the 50 years from 1963 to 2012 were tropical storms or category 1 hurricanes at landfall (Rappaport 2014), and the Saffir–Simpson scale does not provide an accurate estimate of potential damage for a TC post-landfall (Senkbeil and Sheridan 2006). While a TC's wind speed over land is typically much weaker than over the ocean (Sparks 2003), the rainfall threat may still be high post-landfall. Additionally, the area most impacted by extreme rainfall during a particular TC may be both spatially and temporally distinct from the region with the highest winds. These factors point to the need for an alternative means of characterizing and communicating TC rainfall threats.

Hurricane Harvey (2017) and Hurricane Florence (2018) highlighted the hazard posed by TC rainfall and the challenge of effectively communicating this information to the public. Hurricane Florence, for example, approached the East Coast of the United States as a category 4 hurricane, before weakening and making landfall as a category 1 storm. The storm generated extreme rainfall and severe flooding throughout the Carolinas. Over 900 mm of rainfall was recorded in Elizabethtown, North Carolina, breaking the state's record for TC rainfall. There is anecdotal evidence that the downgrade in Florence's category as it approached the coast was perceived by members of the public as an indication of reduced hazard, resulting in some residents choosing not to evacuate (Achenbach and Wax-Thibodeaux 2018).

The previous year, in 2017, Hurricane Harvey stalled over southeastern Texas for several days, making landfall as a category 4 hurricane and weakening to a tropical storm shortly thereafter. Over 1,500 mm of rain fell in Nederland, Texas—the highest TC-related rainfall total ever recorded in the United States. Experts and the media attempted to use recurrence intervals to contextualize the associated rainfall and flooding, with some media outlets

reporting that Harvey was a "500-yr" or "1,000-yr" event (Ingraham 2017; Lind 2017; Samenow 2017), while some outlets noted the shortcomings of these claims (Koerth-Baker 2017; D'Angelo 2017; Bledsoe 2017).

Recurrence interval (i.e., return period) estimates are critical to the fields of engineering design and probabilistic hazard and risk assessment. They are typically estimated by fitting a statistical distribution to a time series of observations (Coles 2001). A rainfall or flood event with a 500-yr recurrence interval has a 1 in 500 (0.2%) probability of being exceeded in any year (i.e., annual exceedance probability); such an event will occur, on average, once every 500 years in a stationary (i.e., unchanging) climate. The usage of these statistical measures is complicated by the fact that storm duration is a critical component in determining the impacts of an extreme rainfall event. A 1-day, 500-yr rainfall event could generate localized flash flooding, for example, while a 3-day, 500-yr event could cause widespread flooding in large watersheds. Previous attempts to develop TC classification systems have highlighted how differences in storm duration result in different magnitudes of TC impacts (Senkbeil and Sheridan 2006).

Rainfall records are rarely longer than 75 years in the United States and are considerably shorter in many other parts of the world. Thus, rainfall recurrence interval estimates tend to be subject to substantial sampling uncertainty because the period of record is often substantially shorter than the desired quantile. Rainfall distributions are typically derived from point-scale observations (such as rain gauges), describing the distribution of extreme rainfall at a specific location, but with a limited ability to describe distributions at larger spatial scales. Additionally, when new events occur that lie outside the range of previously observed rainfalls, recurrence interval estimates should, in principle, be updated to reflect these new records. These changes can be quite large, as seen in the revised Atlas 14 precipitation frequency estimates from the National Oceanic and Atmospheric Administration (NOAA) for the state of Texas, released in September 2018. An earlier estimate of the 100-yr rainfall in Houston, based on rainfall records up to the 1960s, was approximately 330 mm (13 in.) in 24 h (Hershfield 1961); this was updated to 457 mm (18 in.) in Atlas 14 using the most up-to-date data for the region, including observations of rainfall from Harvey (Perica et al. 2018).

In addition to these statistical challenges, recurrence intervals can be confusing and misleading to the public (Keller et al. 2006). Probabilities and frequencies are abstract concepts, creating room for misinterpretation (Schneider 2016). For example, there is a common misperception that multiple 100-yr events cannot occur within a short timeframe. Statistically, however, there is a 26.4% chance of two or more 100-year events of the same duration occurring at a particular location within any century-long period; this issue is complicated even further when events of varying durations are considered. Additionally, the understanding of probabilistic metrics is highly individual—the same metric can have different meanings for different users based on their own perception of risk (Schneider 2016).

A growing number of studies highlight the importance of "experiential processing" in everyday decision-making—the idea that decisions are often made by relating current situations to events that individuals can recall from prior personal experience or recent media reports and images (Marx et al. 2007). Investigations into how individuals process information related to weather hazards have shown some shortcomings of current approaches, including recurrence intervals, and some have proposed alternatives that could convey this information more effectively (Schroeder et al. 2016; Lave and Lave 1991; Wachinger et al. 2013). A survey of residents in a flood-prone community in Texas in the United States, for example, highlighted how residents were more concerned about a potential flooding hazard when concrete information about the nature of flooding was provided, as opposed to abstract probabilities (Bell and Tobin 2007). Preparedness ahead of high-impact floods in 2015 and 2016 in the United Kingdom may have been reduced because residents had trouble adequately

conceptualizing the magnitude of the flooding, which exceeded any that had occurred in recent memory (Cologna et al. 2017).

The extreme rainfall multiplier

Given these documented shortcomings with existing methods, we propose four requirements that should be considered when developing an ideal "scale" to quantify and communicate TC rainfall hazard:

1) The scale must accurately characterize TC rainfall hazard.
2) The scale should identify "locally extreme" rainfall events, based on the recognition that local negative impacts increase in conjunction with increasing positive deviations from the local rainfall climatology.
3) The scale should succinctly describe TC rainfall hazards of various durations by identifying the threats posed by extreme rainfall at a range of time scales up to the lifetime of the storm system.
4) The scale should have an easy-to-understand meaning rooted in experiential processing to ensure efficacy in communicating the TC rainfall hazard to the public.

We use the extreme rainfall multiplier (ERM) as a metric for TC rainfall hazard that can satisfy these requirements. For storm s and location x, the rainfall depth over duration t can be written as $R_{s,x,t}$ and

$$\mathrm{ERM}_{s,x,t} = \frac{R_{s,x,t}}{R_{x,t}^{T\text{-yr}}}.$$

The denominator $R_{x,t}^{T\text{-yr}}$ is the rainfall depth for the T-yr average recurrence interval for the same location and duration. To our knowledge, this concept was first applied to river flood peaks instead of rainfall extremes in Smith et al. (2018), using the name "upper-tail ratio," though the practice of normalizing extreme rainfall and flood observations by a more frequent quantile has longstanding precedent in hydrologic practice, including so-called "index flood"–based estimation of rainfall and flood quantiles using regional observations (e.g., Stedinger et al. 1993). Other metrics, such as the "wet-millimeter day" (Shepherd et al. 2007), have attempted to quantify extreme TC rainfall via quantitative comparison to a reference value.

In this study, we use the 2-yr rainfall event as the denominator in the above equation, to represent a baseline "heavy" rainstorm that would occur relatively frequently. The 2-yr rainfall represents the median annual maximum rainfall—the median value in a time series of the largest rain events per year, based on recent climatology—and, statistically has a 50% chance of being exceeded in any given year. In hydrologic engineering, the 2-yr flood event is often considered a reasonable approximation of the threshold above which floodwaters overflow stream banks and negative impacts begin (Leopold 1968). This "rule of thumb" suggests that events below the 2-yr rainfall (e.g., ERM < 1.0) generally will not produce negative impacts, while those above the 2-yr rainfall (e.g., ERM > 1.0) may. The 2-yr rainfall has the added statistical advantage that, unlike more extreme quantiles, it is easier to estimate accurately and is less prone to fluctuate as additional extreme events are added to the observational record, making it a more "stable" normalization factor with less need for frequent updating. (The sidebar contains additional information about how the 2-yr rainfall is defined and calculated.)

An individual may struggle to understand the event magnitude associated with a rare event (such as a 500-yr rainfall), particularly if a such an event has not occurred recently in their location. However, it is likely that an individual has experienced a more typical rainstorm (similar to the 2-yr storm) in the relatively recent past. Intuitive understanding of one's local

climatology can therefore serve as an "anchor," which, in cognitive psychology research, is an initial piece of information upon which subsequent judgements are based (Tversky and Kahneman 1974). Expressing the magnitude of rare events as multiples of this anchor, which is derived from local climatology rather than abstract probabilities, can help the public utilize their own experiences to conceptualize the magnitude of extreme events.

Analysis of historical tropical cyclone ERMs

A total of 385 North Atlantic TCs that made landfall or passed within 500 km of the eastern United States between 1948 and 2017 were analyzed for this study. NOAA's gridded, gauge-based CPC-Unified dataset (Xie et al. 2007, 2010; Chen et al. 2008) was the source of precipitation data for this analysis. The CPC-Unified dataset contains precipitation information for the continental United States (CONUS) at a spatial resolution of 0.25° × 0.25° (approximately 600 km^2) and a temporal resolution of 1 day. The CONNECT algorithm (Sellars et al. 2015; see appendix for details) was used to convert the gridded precipitation data into four-dimensional precipitation objects, identifying over 12,000 unique rainfall events. To narrow this database, historical TC tracks from NOAA's HURDAT-2 were used to identify the objects associated with North Atlantic TCs that made landfall (or passed near) the continental United States (see appendix for details).

Defining a "typical" heavy rainfall event

The ERM metric is useful because it normalizes extreme rainfall events in the context of the rainfall climatology at particular locations. Compared to using event total rainfall, ERM allows for a more detailed comparison of the relative severity of rainfall events between locations, focusing not solely on the sheer magnitude of the event, but on how much it deviates from typical rainfall events. Compared to other metrics of precipitation climatology—such as daily precipitation records or monthly or seasonal climate normals—ERM is calculated independent of date of occurrence, allowing for events from different times of the year to be compared.

However, selecting the appropriate value for the normalizing factor (the denominator of the ERM equation) involves several important considerations, particularly in terms of the time period used to estimate the 2-yr rainfall. Statistically, it is generally desirable to use the longest data record possible when generating recurrence interval estimates; the uncertainty of recurrence interval estimates typically decreases as the period of record increases. However, this is not necessarily true when nonstationarity exists within the data. Based of CPC-Unified rainfall data, there are statistically significant positive linear trends (p values much less than 0.05) for the mean 2-yr rainfall amount across much of the United States and within the geographic regions considered in this study, for all rainfall durations between 1 and 7 days. This implies that rainfall observations from earlier in the CPC-Unified record may be less representative of present-day "typical" heavy rainfall events.

To solve this issue, we propose that ERM be calculated similarly to the well-known concept of "climate normals," as defined by the World Meteorological Organization (World Meteorological Organization 2017). Climate normals for ERM were calculated by determining the median (i.e., 2-yr) annual maximum rainfall for each grid cell for the 30-yr period from 1981 to 2010. This has the added advantage of making ERM similar to other climate normals the general public may already familiar with; for instance, current normal high and low temperatures are also based on the 1981–2010 reference time period. Additionally, using of the median, rather than the mean, of annual maximum rainfall minimizes the impact of outlier events in determining the climate normals (e.g., Arguez and Vose 2011).

CPC-Unified was also used to estimate the 2-yr rainfall for each grid cell. Using these values, daily and multiday rainfall totals, up to the lifetime of each storm, were converted into their corresponding ERM. The single grid cell from each cyclone with the highest ERM (regardless of duration) was selected for additional analysis (referred to hereafter as "single-cell storm maximum ERM"). Single-cell ERMs were used here for simplicity and because of their resemblance to how TCs are currently classified by maximum sustained wind speed (which usually exists over a relatively small region of a TC) using the Saffir–Simpson scale. Analysis of the area (or the number of grid cells) exceeding certain ERM thresholds could be another way of quantifying extreme TC rainfall events, which often produce spatially extensive rainfall (Stevenson and Schumacher 2014).

The overall distribution of single-cell storm maximum ERM is shown in Fig. 1, along with distributions of these values by the associated rainfall duration and TC strength based on the

Saffir–Simpson scale. While the mean single-cell storm maximum ERM is approximately 2.0, the distribution features multiple high-impact TC rainfall events. Nineteen TCs (4.8%) have ERM values greater than 4, including Hurricane Harvey (2017), which has an ERM maxima of 6.4—the highest value found within the TC database. This indicates that the rainfall from Hurricane Harvey was more than 6 times greater than the typical heavy (2-yr) rainfall event at that location (Fig. 2).

The large majority (74.0%) of single-cell storm maximum ERM values are associated with rainfall durations of 1 day, highlighting how TCs only occasionally become long-lived rainfall events. The distribution of these ERM values by duration highlights that high ERM events occur at both daily and multiday time scales (Fig. 1b). There is a weak but statistically significant correlation between storm maximum ERM and event duration (Kendall's tau rank correlation of 0.125; $p = 0.002$). When classified by peak Saffir–Simpson category at (or near) initial U.S. landfall, there is a positive relationship between Saffir–Simpson wind speed categories and single-cell storm maximum ERM (Fig. 1c; Kendall's tau rank correlation of 0.324; $p < 10^{-1}$).

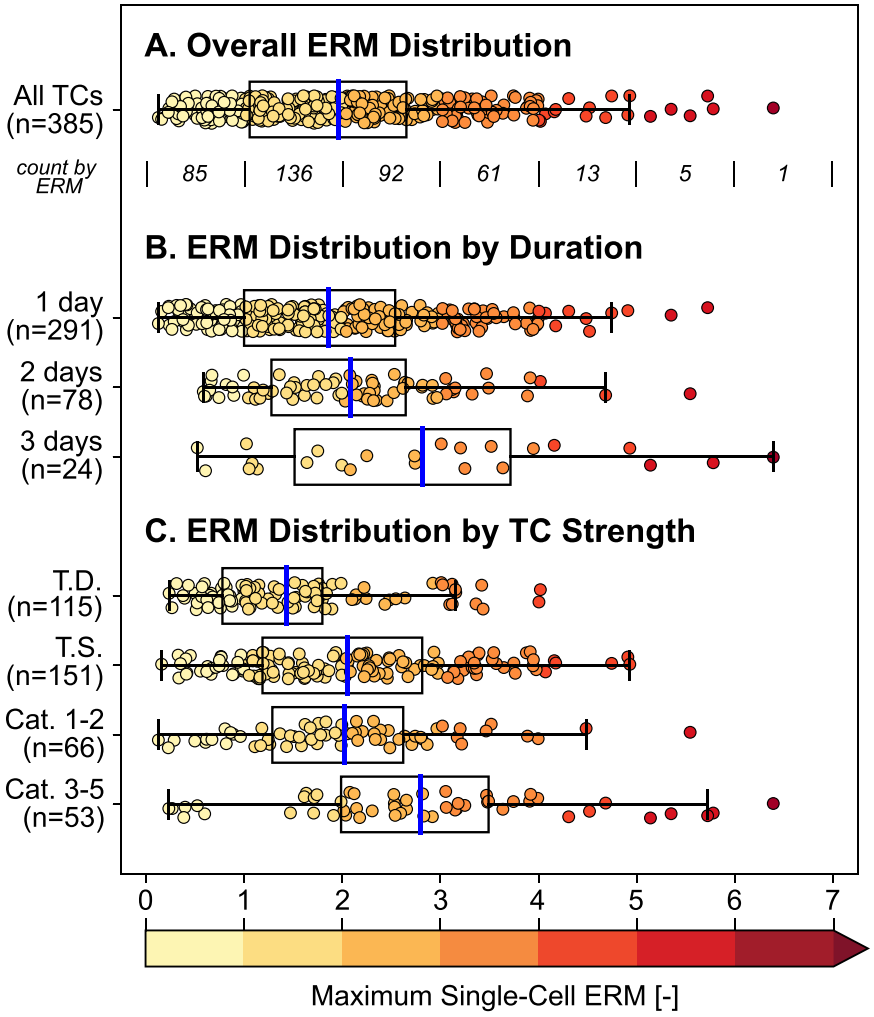

Fig. 1. (a) Overall distribution of single-cell maximum ERM, (b) distribution of ERM based on rainfall duration associated with ERM maxima, and (c) distribution of ERM based on peak TC strength (based on Saffir–Simpson scale) within 500 km of location of initial TC landfall in the CONUS. Blue lines indicate the mean for each distribution.

Deeper examination of three TCs with the highest ERM values in three regions of the United States highlights some of ERM's properties. As mentioned previously, Hurricane Harvey produced the largest ERM (6.4) since 1948, near Giddings, Texas. This ERM was the result of 565 mm of rainfall over a 3-day period, a value 6.4 times greater than the 3-day, 2-yr rainfall (88 mm) in that grid cell. Because CPC-Unified data represent a spatial average over a 0.25° grid cell and is interpolated from rain gauges, the rainfall total for this grid cell is lower than some individual gauge measurements from Hurricane Harvey. Additionally, this grid cell represents the location where Harvey's rainfall deviated most from the local rainfall climatology, which is not necessarily collocated with the place of highest rainfall. (An ERM value above 6.0 was also found near Houston, Texas, associated with CPC-Unified rainfall of 787 mm.)

Hurricane Georges made its final landfall near Biloxi, Mississippi, on 28 September 1998 as a category 2 storm. Within 24 h, the system weakened to a tropical depression and became nearly stationary. Georges generated 561 mm of rain in 2 days near Andalusia, Alabama, resulting in a single-cell maximum ERM of 5.5. Hurricane Floyd first came ashore in North Carolina as a category 2 storm on 16 September 1999. A particularly large storm, Floyd left 415

mm of rainfall in 1 day near Bald Head Island, North Carolina, producing a single-cell maximum ERM of 5.7. These results highlight that very high ERM values can occur at a range of rainfall durations and geographic locations.

We computed the ERMs for durations ranging from 1 to 3 days to further demonstrate the relationship between ERM and rainfall duration. At the 1-day duration, the ERM for Hurricane Harvey near Giddings, Texas is less than 4.0, climbing to over 5.0 at the 2-day duration before reaching its maximum of 6.4 at 3 days (Fig. 3a). The ERM for Georges, in contrast, peaks at 2 days but remains above 5.0 for the 3-day duration (Fig. 3b). As a system that quickly moved up the East Coast of the United States, the ERM for Floyd peaks at 1-day duration and declines slightly at the 2-day duration (Fig. 3c).

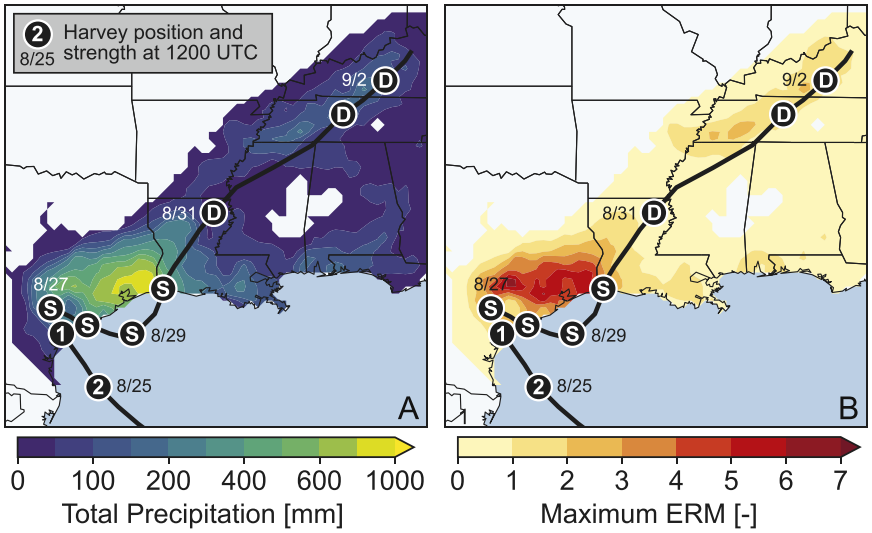

Fig. 2. (a) Storm total precipitation, based on CPC-Unified data and CONNECT precipitation objects, for Harvey (2017). (b) Maximum ERM values for locations with rainfall associated with Harvey (2017). Black lines show the HURDAT-2 storm track. Black circles highlight the 1200 UTC position of Harvey. Characters inside black circles represent 1200 UTC intensity of Harvey (D: tropical depression; S: tropical storm; 1–5: hurricane, with Saffir–Simpson category).

These three storms generated significant impacts in the continental United States. Hurricane Harvey caused $125 billion in damages (second only to Hurricane Katrina) and 68 deaths in Texas; 65 of these deaths were attributed to freshwater flooding (Blake and Zelinsky 2018). Hurricane Georges was responsible for $3.8 billion in damages and one direct death in the United States, which was linked to freshwater flooding (Guiney 1999). Hurricane Floyd caused $9.6 billion in damages and 56 direct deaths in the United States, most of which were caused by freshwater flooding (Pasch et al. 1999). [All TC damage figures are inflation-adjusted to

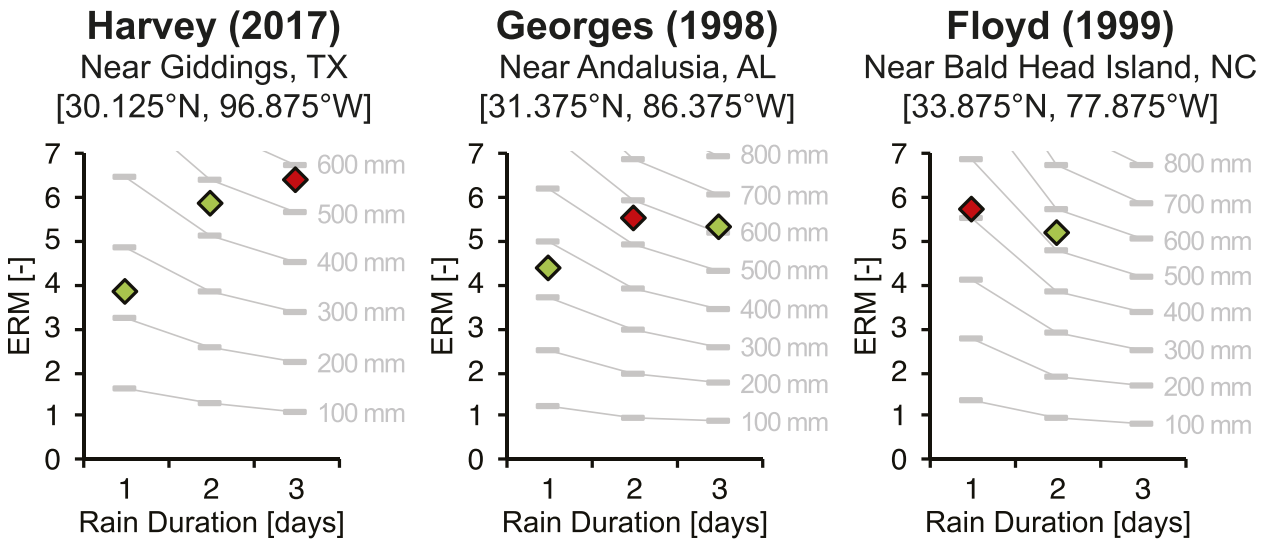

Fig. 3. Comparison of location-specific ERM values (*y* axis), rainfall (gray isolines and gray markers), and associated single-cell TC ERM values (green diamonds; red diamonds show the ERM-maximizing duration) for varying durations for (left) Harvey (2017), (center) Georges (1998), and (right) Floyd (1999). Rainfall for Floyd did not last beyond 2 days at that location, and thus the 3-day ERM for that storm is omitted.

2017 and are from the National Hurricane Center's 2018 update of estimates from Blake et al. (2011).] The correspondence between high ERM and high storm impacts for these three TCs, despite their relatively low Saffir–Simpson categories at the time of rainfall impact, lends support to the suitability of ERM as a metric for characterizing TC rainfall hazard.

Regional distribution of tropical cyclone upper-tail ratios

Figure 4 shows the single highest ERM for each 0.25° grid cell in the eastern and southern United States that has experienced at least one TC rainfall event from 1948 to 2017. While ERM values generally decrease with distance from the coast, there is a wide geographic distribution of high ERM values throughout the analyzed region.

Empirical probability density functions (Fig. 5a) and inverse cumulative distribution functions (Figs. 5b–d) of single-cell storm maximum ERM were constructed to compare the historical distributions of this metric in three regions of the United States subject to TC rainfall extremes: the Texas–Louisiana area of the Gulf Coast, the rest of the Gulf Coast and the inland southeast (including Florida and Georgia), and the remaining states along the Atlantic Coast. Due to topographic and climatic features, these three regions differ in terms of the types and paths of TCs that make landfall (Elsner et al. 2000; Matyas 2013). Despite such differences, the distributions of single-cell storm maximum ERMs for the regions shown in Fig. 5 are remarkably similar. These results suggest that the distribution of ERM maxima is relatively invariant to geographic location. This property would allow for hazard communication to be placed within the context of the local rainfall hydroclimate, despite

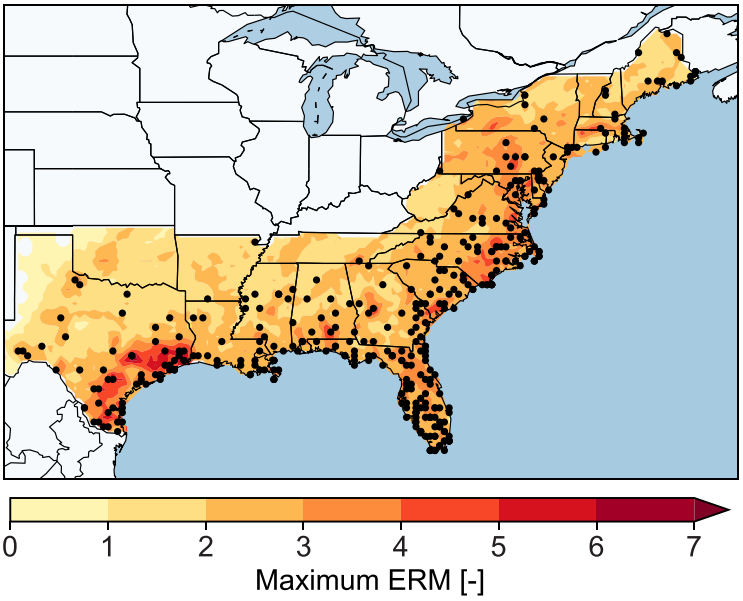

Fig. 4. Map of maximum ERM for grid cells in coastal regions of the United States experiencing rainfall from at least one North Atlantic TC. Locations of single-cell storm maximum ERM values are marked by black dots.

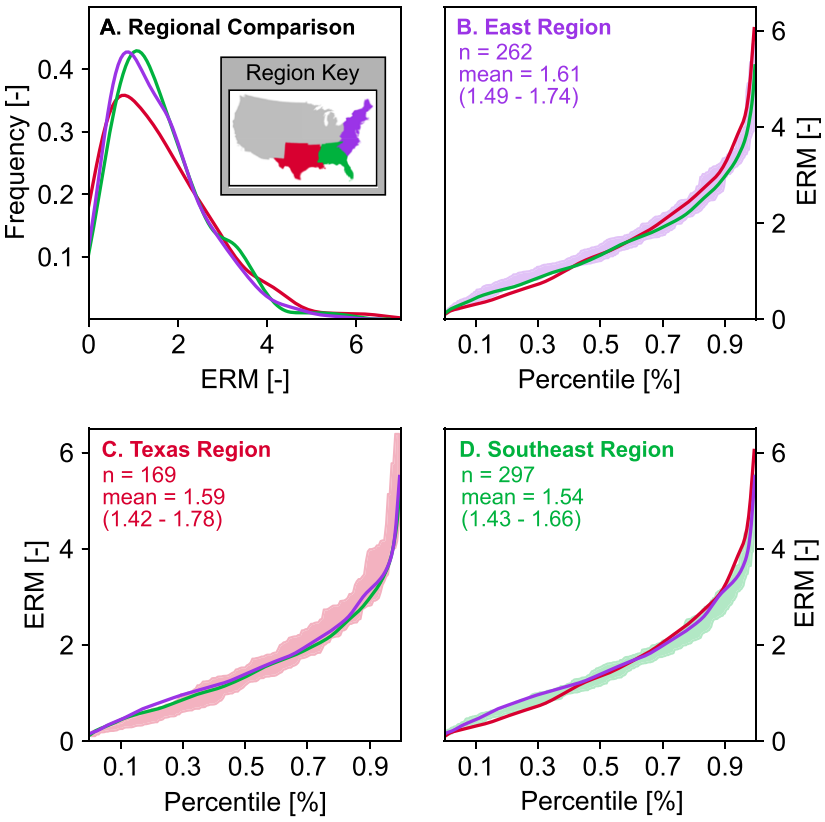

Fig. 5. (a) Empirical probability density functions of regional distributions of single-cell storm maximum ERM for North Atlantic TCs, based on Gaussian kernel density estimates. (b)–(d) Empirical inverse cumulative distribution functions of single-cell storm maximum ERM by region; some TCs produced maxima in multiple regions. Colored shading represents 95% confidence intervals derived via nonparametric bootstrapping. Regional means are also displayed as inset text; values in parentheses represent 95% confidence intervals of these means, also derived via nonparametric bootstrapping. Inset map in (a) identifies regions used for subsequent analysis.

significant differences in the extreme rainfall hydroclimatology throughout the eastern United States. This property also facilitates estimation of ERM annual exceedance probabilities, described in the next section.

Estimating the climatological frequency of high ERM events

As shown above, the distribution of single-cell storm maximum ERM is practically invariant to geographic location (Figs. 4 and 5) and only moderately sensitive to duration (Fig. 1b). These properties imply that a single statistical distribution can approximate ERM over the eastern and southern United States for all storm durations. Such a distribution could be useful to the hydrologic hazard and risk assessment communities since it could yield estimates of the recurrence intervals of past or future TC rainfall events. In addition, if recurrence intervals are to be used in public communication, estimates derived from this ERM distribution may prove more effective, as we argue below.

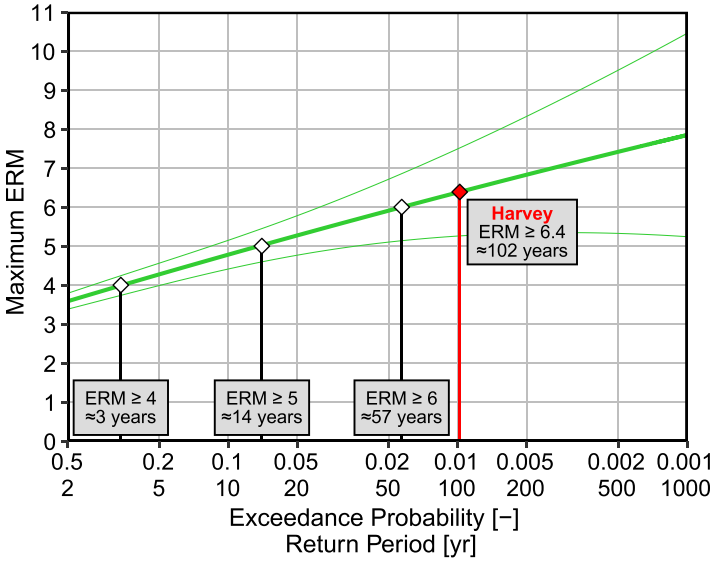

Fig. 6. Plot of recurrence intervals for the fitted POT extreme-value model. The red diamond indicates the recurrence interval corresponding to the storm maximum ERM of 6.4 from Hurricane Harvey. White diamonds indicate the recurrence interval of TC rainfall events with storm maximum ERMs greater than or equal to listed thresholds within the United States. Green lines indicate the 90% confidence interval of ERM as a function of recurrence interval.

A peaks-over-threshold (POT) extreme value model was fitted using the 385 single-cell storm maximum ERM values in order to estimate the frequency of TC rainfall events that exceed a range of ERM values within the eastern and southern United States (Fig. 6; see appendix for details on extreme value modeling and Fig. 4 for the region of analysis). In developing this model, normalizing TC rainfall totals by the 2-yr rainfall is statistically beneficial since it reduces the variance and skewness of ERM relative to "raw" (i.e., non-normalized) rainfall values. For example, the coefficient of variation (skewness) reduces from 0.68 (1.50) for the rainfall time series to 0.58 (0.78) for the ERM time series (Fig. 7). (Coefficient of variation is the sample standard deviation divided by the sample mean). Lower values of these higher-order statistical moments generally lead to more robust parameter estimates and inferences.

Based on this model, a TC rainfall event with an ERM of 4.0 or higher would be expected to occur approximately once every 3 years somewhere in the study region. Events with ERMs exceeding 5.0 and 6.0 have recurrence intervals of roughly 13 and 57 years, respectively. A TC with an ERM magnitude equal or greater to Hurricane Harvey (ERM ≥ 6.4) has an estimated recurrence interval of approximately 102 years.

It is important to note, however, that the model shown in Fig. 6 provides the recurrence intervals or annual exceedance probabilities of events occurring *anywhere* within the study region shown in Fig. 4. This is in contrast with the common usage of recurrence intervals to describe event likelihood at a specific location. While the likelihood of an extreme event like Hurricane Harvey occurring at any specific location—such as the Houston metropolitan area—is very low, the probability of an event of this magnitude occurring somewhere within the eastern United States may be considerably higher. This distinction is probably lost on many members of the public, which may contribute to further confusion when recurrence interval terminology is used in the popular media. If recurrence intervals are to be used to contextualize individual events (as they were in the popular media during and after Hurricane Harvey), it may be more appropriate to report them based on "regional recurrence" estimates like those presented in Fig. 6.

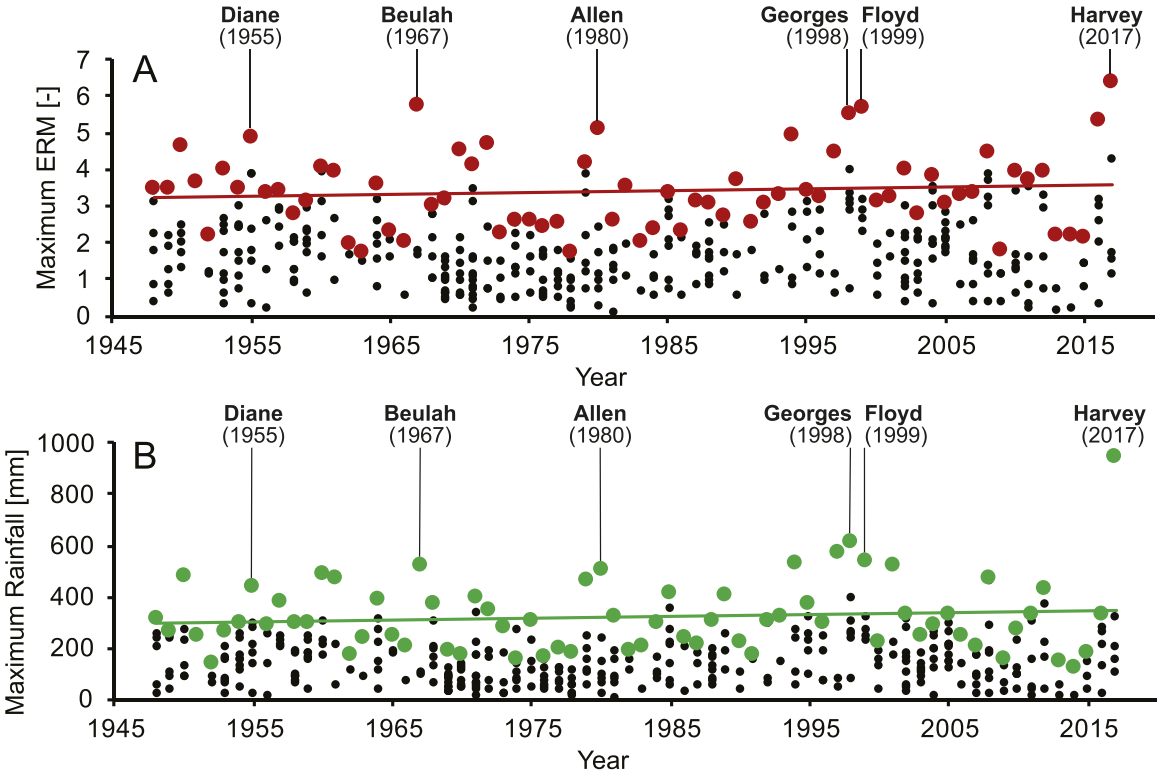

Fig. 7. Time series of (a) maximum single-cell ERM and (b) rainfall for all TCs, 1948–2017. Highest values per year indicated with colored markers. Colored lines represent linear regression fit for annual maxima time series. A Mann–Kendall test for monotonic trends in annual maxima values did not reveal significant changes over time for either ERM (z = 0.441, n = 70, p = 0.659) or rainfall (z = 0.203, n = 70, p = 0.839).

In contrast, it is not defensible to compute regional recurrence estimates based on rainfall observations themselves, since the rainfall distributions at individual locations in the study region—for instance, Texas and New Jersey—differ substantially. Meanwhile, the regional invariance of ERM demonstrated in the "Regional distribution of tropical cyclone upper-tail ratios" section means that it is defensible to consider all ERM events as belonging to a single population, thus increasing sample size and permitting robust regional recurrence estimation.

Using this property of regional invariance, it may also be possible to develop models to estimate the recurrence interval of high-ERM events with extensive geographic footprints; the large spatial extent of Hurricane Harvey's extreme rainfall was major contributor to its catastrophic impacts. With this information, recurrence interval estimates of ERM extent could be derived, which may have utility in specific forecasting or risk assessment applications.

Using ERM to communicate a TC rainfall forecast

To demonstrate how ERM could be used in a forecast setting, ERM values for Hurricane Florence were calculated from 5-day quantitative precipitation forecasts (QPFs) issued by NOAA's National Weather Service Weather Prediction Center (WPC) before the storm made landfall. More details on these forecasts and how ERM values were computed for them are found in the appendix. Forecasts issued by the National Hurricane Center called for Florence to approach the North Carolina coast as a major hurricane. However, Florence weakened more rapidly than expected, ultimately making landfall as a category 1 system. The resulting wind-related impacts, while severe, were less than originally anticipated.

In contrast to the wind hazard, forecast ERM for Hurricane Florence indicates that the expected rainfall hazard was very high, and increasing, as the storm neared the United States. Estimates of the peak, single-cell, 5-day ERM for Hurricane Florence increased from 4.2 on 12 September (Fig. 8a) to 5.0 on 14 September (Fig. 8b). The estimated 3-day ERM on the day

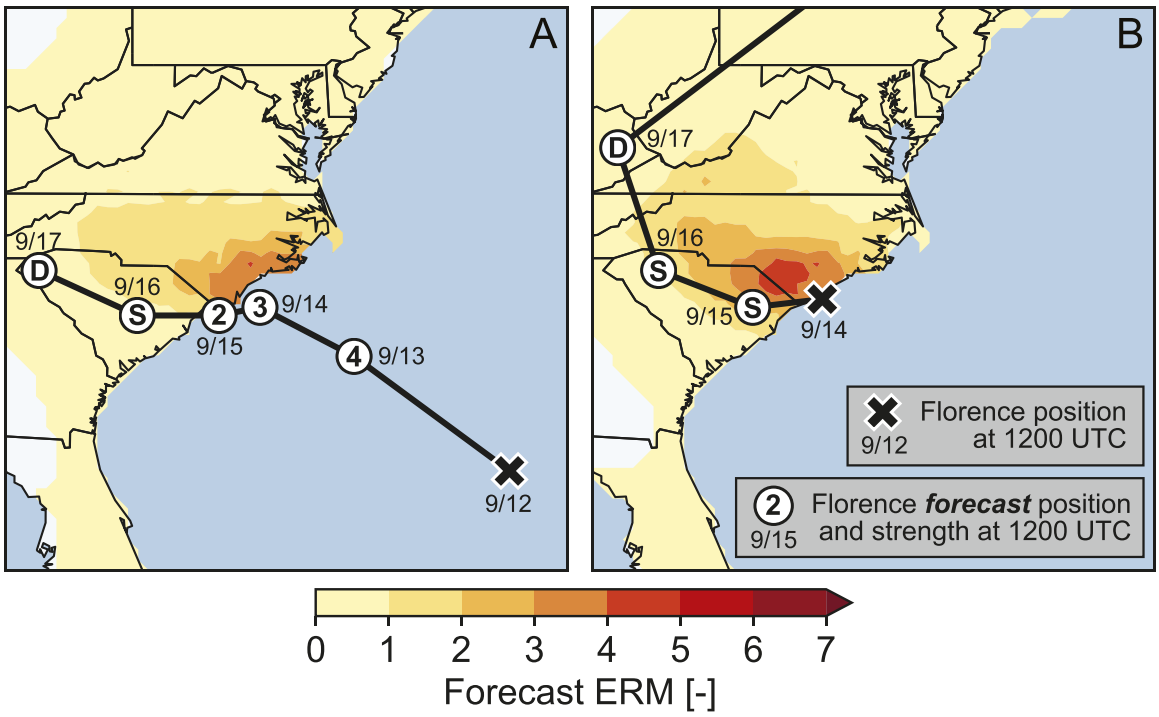

Fig. 8. Five-day ERM forecasts based on QPF estimates issued at (a) 1200 UTC 12 Sep 2018 and (b) 1200 UTC 14 Sep 2018. Peak forecast ERM values are 4.2 in (a) and 5.0 in (b). White circles indicate National Hurricane Center (NHC) forecast TC track positions on date of rainfall forecast. Characters inside white circles represent NHC forecast intensity of Florence (D: tropical depression; S: tropical storm; 1–5: hurricane, with Saffir–Simpson category).

of Florence's landfall was even higher at 5.7 (not shown). Not only did these forecast ERM values remain elevated amid Florence's weakening winds, the magnitude of these forecast ERM values is extremely high. A value of 5.7 would equal Hurricane Floyd (1999) as the highest ERM value ever seen on the Atlantic coast, and the second-highest ERM value anywhere since 1948 (after Hurricane Harvey). Additionally, while this study has focused primarily on the single-cell storm maximum ERM, the forecast maps (Figs. 8a,b) show how the spatial extent of rainfall hazard could be communicated to the public using ERM. Areas of 19,700 and 33,700 km^2 have forecast ERMs greater than 3.0 on 12 and 14 September, respectively.

These forecast ERM values were validated using poststorm CPC-Unified rainfall observations. The single-cell storm maximum ERM based on CPC-Unified was found near Lumberton, North Carolina, where a 2-day rainfall total of 472 mm generated an ERM value of 5.8. Throughout the Carolinas, a region of 36,900 km^2 experienced an ERM above 3.0. Verification of the original rainfall forecast from the National Weather Service (and the ERM values derived from it) for the 3-day period after the landfall of Hurricane Florence can be seen in Fig. 9. It should be noted, however, that the utility of any ERM forecast in this context is dependent on the accuracy of the rainfall forecast used to generate ERM values.

When compared to current forecast products and to recurrence interval estimates, ERM forecast values can contextualize extreme QPF values and potentially provide a more tangible meaning to the public. Forecast ERM values can be compared to past rainfall events to find similarly extreme historical analogs; doing so might allow communicators to develop appropriate "indexical images"—real-world depictions of possible damages. This type of imagery has been shown to lead to higher risk perception (Rickard et al. 2017) and highlight another way ERM could be used to identify and communicate potential rainfall hazard in the days before TC landfall. At least one existing rainfall hazard product utilized during TC events—the Excessive Rainfall Outlook (ERO) issued by the WPC—focuses on the probability of rainfall exceeding flash flood thresholds, emphasizing the likelihood rather than the magnitude of

the rainfall threat. ERM could be used as a complement or alternative to these outlooks.

Summary and conclusions

We have demonstrated that the extreme rainfall multiplier (ERM) framework to quantify TC rainfall offers several useful properties. When applied retrospectively, it produces values that correspond with observed TC rainfall impacts for several high-impact events, confirming that it can depict hazard. ERM values reflect geographic differences in the climatology of rainfall extremes and can succinctly describe TC rainfall hazard of varying durations using a single scale. Furthermore, an ERM value has an intuitive interpretation that leverages individuals' conceptions and prior experiences of rainfall magnitudes, lending itself to communicating TC rainfall hazard and contextualizing recent and imminent TC rainfall extremes for the public. The ERM framework could be applied to rainfall extremes produced by TCs in other basins (particularly eastern Pacific TCs, which can cause high impacts from extreme rainfall in the southwestern United States), to other types of rainfall-producing storm systems, and, in principle, to other types of natural hazards.

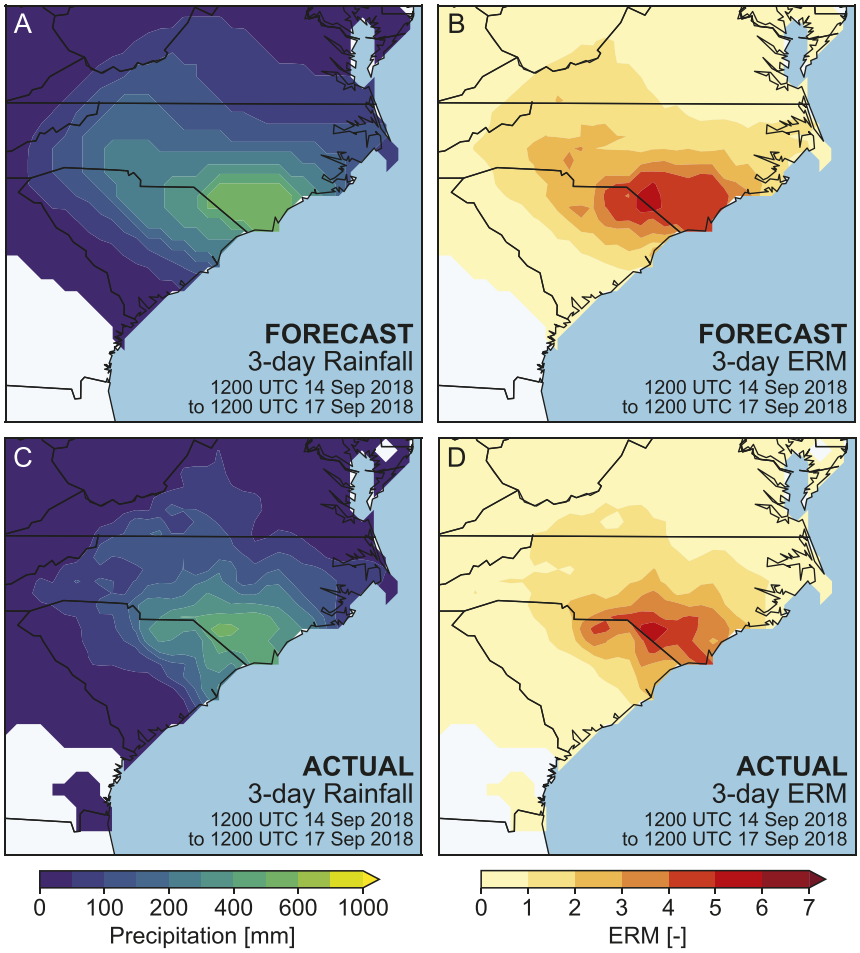

Fig. 9. (a) Three-day forecast rainfall based on QPF estimates issued at 1200 UTC 14 Sep 2018 and (c) actual rainfall based on CPC-Unified data. (b) ERM forecasts derived from QPF estimates and (d) ERM based on poststorm CPC-Unified data.

Despite observational evidence for increasing TC intensity (Emanuel et al. 2006) and decreases in translational speed (Kossin 2018), relatively less work has been done to assess changes in TC rainfall hazards (Emanuel et al. 2006; Langousis and Veneziano 2009; Kunkel et al. 2010). Challenges facing TC rainfall trend studies are the limited observations available at any particular location as well as the influences of geographically varying rainfall hydroclimate and storm lifetime. The relative invariance of ERM to geographic location is a potentially useful property for investigation of TC rainfall nonstationarity, allowing for the construction of time series using all TCs within an entire region, rather than only those at particular locations. However, we found no evidence of nonstationarity in either ERM or the underlying rainfall totals used to compute it (Fig. 7); more work is needed.

A number of issues must be resolved before ERM could be suitable as an operational forecast communication product. These include the differences in the resolution and coverage of gridded rainfall products and precipitation forecasts, how and whether to communicate a range of forecast lead times or durations, and what graphical and verbal techniques should be used to communicate it most effectively. Nonetheless, our Hurricane Florence ERM "hindcast" demonstration showed that the method is able to accurately characterize the rainfall hazard

of a significant TC event several days before the impacts were realized, in a way that could be readily communicated to, and interpreted by, the public.

Acknowledgments. C.D.B. and D.B.W. were partially supported by the U.S. National Science Foundation Hydrologic Sciences Program (CAREER Award EAR-1749638) and by the University of Wisconsin–Madison.

Appendix: Detailed methods

Converting gridded data into precipitation objects. The CONNECT algorithm was used to convert NOAA's gridded, gauge-based CPC-Unified precipitation data into precipitation objects (Sellars et al. 2015). The algorithm connects the precipitation data based on the underlying relationships within individual data observations in four dimensions: latitude, longitude, time, and rainfall intensity. To minimize spurious connectivity from the object generation process, observations of rainfall intensity less than 10 mm day^{-1} are not included in the connectivity analysis. Observations that are connected in at least one dimension of the analysis (i.e., that are connected spatially and/or temporally) are joined together to create a precipitation object, which depicts the evolution of precipitation over space and time (Sellars et al. 2013). Applying this algorithm to the CPC-Unified dataset created over 12,000 unique precipitation objects for the period 1948–2017, each representing a historical rainfall event.

Pairing precipitation objects with historical TC tracks. The complete precipitation object database generated from the CPC-CONNECT database contains historical rainfall events of multiple types, throughout each year. To narrow this database, historical TC tracks were used to identify the objects associated with North Atlantic TCs that made landfall (or passed near) the continental United States. Hurricane storm track data were obtained via NOAA's HURDAT-2 Atlantic hurricane database, which reports the 6-h position (latitude and longitude) of North Atlantic TCs, as well as maximum wind speed and central barometric pressure (Landsea and Franklin 2013). TC tracks that made landfall or passed within 500 km of the continental United States were used in subsequent analyses. [Distances of 500 km have been used in previous studies to identify rainfall and flooding associated with TCs (Hart and Evans 2001; Lonfat et al. 2004; Zhou and Matyas 2017).] Precipitation objects that pass concurrently within 500 km of one of these storm tracks were identified. A total of 385 storm tracks that were associated with one (or more) rainfall precipitation object(s) in the eastern United States from 1948 to 2017.

Extreme value modeling. The peaks-over-threshold (POT) generalized Pareto (GP) distribution extreme-value model (Fig. 6) was fitted using maximum likelihood estimation via the *fevd* function from the "extRemes" R package (Gilleland and Katz 2016). This GP model was then used to estimate ERM recurrence intervals. A threshold level of ERM = 3.0 was used, based on visual assessment of diagnostic plots provided by the extRemes package.

Generating ERM forecasts for Hurricane Florence. QPF data were obtained as shapefiles from the data archive of the National Weather Service's Storm Prediction Center (SPC). The forecasts used were issued at 1200 UTC 12 and 14 September 2018, and contained days 1–3 (3-day), days 1–5 (5-day), and days 1–7 (7-day) QPFs for the United States. Each shapefile saved the forecast precipitation data as contours; we transformed these contours to match the 0.25° grid resolution of the CPC-Unified precipitation data. For this analysis, each 0.25° grid cell was assigned the rainfall forecast value equal to the highest contour that was found within (or surrounding) it. These QPFs were then converted into ERM forecasts by dividing by the 2-yr rainfall (based on CPC-Unified) for the appropriate duration.

References

Achenbach, J., and E. Wax-Thibodeaux, 2018: Hurricane Florence, 'just a Cat 1,' reveals flaw with Saffir-Simpson scale. *Washington Post*, 19 September, https://wapo.st/2JjQmZd.

Arguez, A., and R. S. Vose, 2011: The definition of the standard WMO climate normal: The key to deriving alternative climate normals. *Bull. Amer. Meteor. Soc.*, **92**, 699–704, https://doi.org/10.1175/2010BAMS2955.1.

Bell, H., and G. Tobin, 2007: Efficient and effective? The 100-year flood in the communication and perception of flood risk. *Environ. Hazards*, **7**, 302–311, https://doi.org/10.1016/j.envhaz.2007.08.004.

Blake, E. S., and D. A. Zelinsky, 2018: Hurricane Harvey (AL092017). National Hurricane Center Tropical Cyclone Rep., 77 pp., www.nhc.noaa.gov/data/tcr/AL092017_Harvey.pdf.

——, C. W. Landsea, and E. J. Gibney, 2011: The deadliest, costliest, and most intense United States tropical cyclones of from 1851 to 2010 (and other frequently requested hurricane facts). NOAA Tech. Memo. NWS NHC-6, 47 pp., www.nhc.noaa.gov/pdf/nws-nhc-6.pdf.

Bledsoe, B., 2017: We still don't know how to talk about floods. *Washington Post*, 13 September, accessed 21 November 2018, www.washingtonpost.com/news/capital-weather-gang/wp/2017/09/13/we-still-dont-know-how-to-talk-about-floods/.

Chen, M., W. Shi, P. Xie, V. B. S. Silva, V. E. Kousky, R. W. Higgins, and J. E. Janowiak, 2008: Assessing objective techniques for gauge-based analyses of global daily precipitation. *J. Geophys. Res.*, **113**, D04110, https://doi.org/10.1029/2007JD009132.

Coles, S., 2001: *An Introduction to Statistical Modeling of Extreme Values.* Springer, 208 pp.

Cologna, V., R. H. Bark, and J. Paavola, 2017: Flood risk perceptions and the UK media: Moving beyond "once in a lifetime" to "be prepared" reporting. *Climate Risk Manage.*, **17**, 1–10, https://doi.org/10.1016/j.crm.2017.04.005.

D'Angelo, C., 2017: Climate change has "loaded the dice" on the frequency of 100-year floods. *Huffington Post*, 31 August, www.huffpost.com/entry/100-year-flood-climate-change_n_59a6eaa3e4b084581a14ea14.

Elsner, J. B., K. Liu, and B. Kocher, 2000: Spatial variations in major U.S. hurricane activity: Statistics and a physical mechanism. *J. Climate*, **13**, 2293–2305, https://doi.org/10.1175/1520-0442(2000)013<2293:SVIMUS>2.0.CO;2.

Emanuel, K., 2005: Increasing destructiveness of tropical cyclones over the past 30 years. *Nature*, **436**, 686–688, https://doi.org/10.1038/nature03906.

——, S. Ravela, E. Vivant, and C. Risi, 2006: A statistical deterministic approach to hurricane risk assessment. *Bull. Amer. Meteor. Soc.*, **87**, 299–314, https://doi.org/10.1175/BAMS-87-3-299.

Gilleland, E., and R. W. Katz, 2016: extRemes 2.0: An extreme value analysis package in R. *J. Stat. Software*, **72**, 1–39, https://doi.org/10.18637/jss.v072.i08.

Guiney, J. L., 1999: Hurricane Georges (preliminary report). National Hurricane Center, 29 pp., accessed 25 February 2019, www.nhc.noaa.gov/data/tcr/AL071998_Georges.pdf.

Hart, R. E., and J. L. Evans, 2001: A climatology of the extratropical transition of Atlantic tropical cyclones. *J. Climate*, **14**, 546–564, https://doi.org/10.1175/1520-0442(2001)014<0546:ACOTET>2.0.CO;2.

Hershfield, D. M., 1961: Rainfall frequency atlas of the United States: For durations from 30 minutes to 24 hours and return periods from 1 to 100 years. U.S. Weather Bureau Technical Paper 40, 65 pp., www.nws.noaa.gov/oh/hdsc/PF_documents/TechnicalPaper_No40.pdf.

Ingraham, C., 2017: Houston is experiencing its third '500-year' flood in 3 years. How is that possible? *Washington Post*, 29 August, accessed 11 October 2018, www.washingtonpost.com/news/wonk/wp/2017/08/29/houston-is-experiencing-its-third-500-year-flood-in-3-years-how-is-that-possible/.

Keller, C., M. Siegrist, and H. Gutscher, 2006: The role of the affect and availability heuristics in risk communication. *Risk Anal.*, **26**, 631–639, https://doi.org/10.1111/j.1539-6924.2006.00773.x.

Knutson, T. R., and Coauthors, 2010: Tropical cyclones and climate change. *Nat. Geosci.*, **3**, 157–163, https://doi.org/10.1038/ngeo779.

Koerth-Baker, M., 2017: It's time to ditch the concept of '100-year floods.' FiveThirtyEight, 30 August, accessed 8 November 2018, https://fivethirtyeight.com/features/its-time-to-ditch-the-concept-of-100-year-floods/.

Kossin, J. P., 2018: A global slowdown of tropical-cyclone translation speed. *Nature*, **558**, 104–107, https://doi.org/10.1038/s41586-018-0158-3.

Kunkel, K. E., D. R. Easterling, D. A. Kristovich, B. Gleason, L. Stoecker, and R. Smith, 2010: Recent increases in US heavy precipitation associated with tropical cyclones. *Geophys. Res. Lett.*, **37**, L24706, https://doi.org/10.1029/2010GL045164.

Landsea, C. W., and J. L. Franklin, 2013: Atlantic hurricane database uncertainty and presentation of a new database format. *Mon. Wea. Rev.*, **141**, 3576–3592, https://doi.org/10.1175/MWR-D-12-00254.1.

Langousis, A., and D. Veneziano, 2009: Long-term rainfall risk from tropical cyclones in coastal areas. *Water Resour. Res.*, **45**, https://doi.org/10.1029/2008WR007624.

Lave, T. R., and L. B. Lave, 1991: Public perception of the risks of floods: Implications for communication. *Risk Anal.*, **11**, 255–267, https://doi.org/10.1111/j.1539-6924.1991.tb00602.x.

Leopold, L. B., 1968: Hydrology for urban land planning: A guidebook on the hydrologic effects of urban land use. USGS Circular 554, 18 pp., https://doi.org/10.3133/cir554.

Lind, D., 2017: The "500-year" flood, explained: Why Houston was so underprepared for Hurricane Harvey. Vox, 28 August, accessed 8 November 2018, www.vox.com/science-and-health/2017/8/28/16211392/100-500-year-flood-meaning.

Lonfat, M., F. D. Marks, and S. S. Chen, 2004: Precipitation distribution in tropical cyclones using the Tropical Rainfall Measuring Mission (TRMM) Microwave Imager: A global perspective. *Mon. Wea. Rev.*, **132**, 1645–1660, https://doi.org/10.1175/1520-0493(2004)132<1645:PDITCU>2.0.CO;2.

Marx, S. M., E. U. Weber, B. S. Orlove, A. Leiserowitz, D. H. Krantz, C. Roncoli, and J. Phillips, 2007: Communication and mental processes: Experiential and analytic processing of uncertain climate information. *Global Environ. Change*, **17**, 47–58, https://doi.org/10.1016/j.gloenvcha.2006.10.004.

Matyas, C. J., 2013: Processes influencing rain-field growth and decay after tropical cyclone landfall in the United States. *J. Appl. Meteor. Climatol.*, **52**, 1085–1096, https://doi.org/10.1175/JAMC-D-12-0153.1.

Pasch, R. J., T. B. Kimberlain, and S. R. Stewart, 1999: Preliminary Report: Hurricane Floyd. National Hurricane Center, 28 pp., www.nhc.noaa.gov/data/tcr/AL081999_Floyd.pdf.

Perica, S., S. Pavlovic, M. S. Laurent, C. Trypaluk, D. Unruh, and O. Wilhite, 2018: Texas. Precipitation-Frequency Atlas of the United States, Vol. 11, Version 2.0, NOAA Atlas 14, 283 pp., www.nws.noaa.gov/oh/hdsc/PF_documents/Atlas14_Volume11.pdf.

Rappaport, E. N., 2014: Fatalities in the United States from Atlantic tropical cyclones: New data and interpretation. *Bull. Amer. Meteor. Soc.*, **95**, 341–346, https://doi.org/10.1175/BAMS-D-12-00074.1.

Rickard, L. N., J. P. Schuldt, G. M. Eosco, C. W. Scherer, and R. A. Daziano, 2017: The proof is in the picture: The influence of imagery and experience in perceptions of hurricane messaging. *Wea. Climate Soc.*, **9**, 471–485, https://doi.org/10.1175/WCAS-D-16-0048.1.

Samenow, J., 2017: Harvey is a 1,000-year flood event unprecedented in scale. *Washington Post*, 31 August, accessed 21 November 2018, www.washingtonpost.com/news/capital-weather-gang/wp/2017/08/31/harvey-is-a-1000-year-flood-event-unprecedented-in-scale/.

Schneider, S., 2016: Communicating uncertainty: A challenge for science communication. *Communicating Climate-Change and Natural Hazard Risk and Cultivating Resilience: Case Studies for a Multi-Disciplinary Approach*, J. L. Drake et al., Eds., Springer International Publishing, 267–278.

Schroeder, A. J., and Coauthors, 2016: The development of a flash flood severity index. *J. Hydrol.*, **541**, 523–532, https://doi.org/10.1016/j.jhydrol.2016.04.005.

Sellars, S., P. Nguyen, W. Chu, X. Gao, K. Hsu, and S. Sorooshian, 2013: Computational Earth science: Big data transformed into insight. *Eos, Trans. Amer. Geophys. Union*, **94**, 277–278, https://doi.org/10.1002/2013EO320001.

——, X. Gao, and S. Sorooshian, 2015: An object-oriented approach to investigate impacts of climate oscillations on precipitation: A western United States case study. *J. Hydrometeor.*, **16**, 830–842, https://doi.org/10.1175/JHM-D-14-0101.1.

Senkbeil, J. C., and S. C. Sheridan, 2006: A postlandfall hurricane classification system for the United States. *J. Coastal Res.*, **225**, 1025–1034, https://doi.org/10.2112/05-0532.1.

Shepherd, J. M., A. Grundstein, and T. L. Mote, 2007: Quantifying the contribution of tropical cyclones to extreme rainfall along the coastal southeastern United States. *Geophys. Res. Lett.*, **34**, L23810, https://doi.org/10.1029/2007GL031694.

Smith, J. A., A. A. Cox, M. L. Baeck, L. Yang, and P. Bates, 2018: Strange floods: The upper tail of flood peaks in the United States. *Water Resour. Res.*, **54**, 6510–6542, https://doi.org/10.1029/2018WR022539.

Sparks, P. R., 2003: Wind speeds in tropical cyclones and associated insurance losses. *J. Wind Eng. Ind. Aerodyn.*, **91**, 1731–1751, https://doi.org/10.1016/j.jweia.2003.09.018.

Stedinger, J. R., R. M. Vogel, and E. Foufoula-Georgiou, 1993: Frequency analysis of extreme events. *Handbook of Hydrology*, D. R. Maidment, Ed., McGraw-Hill, 18.1–18.66.

Stevenson, S. N., and R. S. Schumacher, 2014: A 10-year survey of extreme rainfall events in the central and eastern United States using gridded multisensor precipitation analyses. *Mon. Wea. Rev.*, **142**, 3147–3162, https://doi.org/10.1175/MWR-D-13-00345.1.

Tversky, A., and D. Kahneman, 1974: Judgment under uncertainty: Heuristics and biases. *Science*, **185**, 1124–1131, https://doi.org/10.1126/science.185.4157.1124.

USGCRP, 2017: *Climate Science Special Report: Fourth National Climate Assessment, Volume I*. D. J. Wuebbles et al., Eds., U.S. Global Change Research Program, 470 pp., https://doi.org/10.7930/J0J964J6.

Wachinger, G., O. Renn, C. Begg, and C. Kuhlicke, 2013: The risk perception paradox—Implications for governance and communication of natural hazards. *Risk Anal.*, **33**, 1049–1065, https://doi.org/10.1111/j.1539-6924.2012.01942.x.

Walsh, K. J., and Coauthors, 2016: Tropical cyclones and climate change. *Wiley Interdiscip. Rev.: Climate Change*, **7**, 65–89, https://doi.org/10.1002/wcc.371.

World Meteorological Organization, 2017: WMO guidelines on the calculation of climate normals. WMO-1203, 18 pp., https://library.wmo.int/doc_num.php?explnum_id=4166.

Xie, P., M. Chen, S. Yang, A. Yatagai, T. Hayasaka, Y. Fukushima, and C. Liu, 2007: A gauge-based analysis of daily precipitation over East Asia. *J. Hydrometeor.*, **8**, 607–626, https://doi.org/10.1175/JHM583.1.

——, ——, and W. Shi, 2010: CPC unified gauge-based analysis of global daily precipitation. *24th Conf. on Hydrology*, Atlanta, GA, Amer. Meteor., Soc., 2.3A, https://ams.confex.com/ams/90annual/techprogram/paper_163676.htm.

Zhou, Y., and C. J. Matyas, 2017: Spatial characteristics of storm-total rainfall swaths associated with tropical cyclones over the Eastern United States. *Int. J. Climatol.*, **37**, 557–569, https://doi.org/10.1002/joc.5021.